Lawrence Berkeley National Laboratory

Title
Surface Energy Anisotropy Effects on Pore-Channel Stability: Rayleigh Instabilities in m-Plane Sapphire

Permalink
https://escholarship.org/uc/item/8fz6768h

Authors
Santala, Melissa K.
Glaeser, Andreas M.

Publication Date
2005-09-07

SURFACE ENERGY ANISOTROPY EFFECTS ON PORE-CHANNEL STABILITY: RAYLEIGH INSTABILITIES IN M-PLANE SAPPHIRE

Melissa K. Santala and Andreas M. Glaeser
Department of Materials Science and Engineering
University of California
&
Ceramic Science Program
Lawrence Berkeley National Laboratory
Berkeley, CA 94720-1760

ABSTRACT

Internal, high-aspect-ratio pore channels with their long axes parallel to the $\mathbf{m}(10\bar{1}0)$ plane of sapphire were generated through sequential application of photolithography, ion-beam etching and solid-state diffusion bonding. The axial orientation of channels within the $\mathbf{m}$ plane was systematically varied to sample a range of bounding-surface crystallographies. The morphologic evolution of these pore channels during anneals at 1700°C was recorded by post-anneal optical microscopy. The development and growth of periodic axial variations in the pore channel radius was observed, and ultimately led to the formation of discrete pores. The wavelength and average pore spacing, assumed to reflect the kinetically dominant perturbation wavelength, varied with the in-plane pore channel orientation, as did the time for complete channel breakup. Results are compared to those previously obtained when pore channels were etched into $\mathbf{c}(0001)$-plane sapphire and annealed under similar conditions. The results indicate a strong effect of surface stability on the evolution behavior.

INTRODUCTION & BACKGROUND

The axial instability of cylindrical high-aspect-ratio phases has been a topic of interest for over a century. The areas of application are remarkably diverse and span a wide range of length scale. As systems with progressively higher surface-to-volume ratio receive increasing interest, particularly in the microelectronics area, it will become ever more important to understand the energetics and kinetics of morphologic instability and to develop effective strategies for stabilizing nanostructures. Thus, interest in this topic is likely to experience a resurgence.

The contributions of Plateau[1] and Rayleigh[2] were critical to understanding the spatio-temporal evolution of cylindrical liquid jets. Plateau showed that cylindrical fluid jets could lower their total surface energy by the development of infinitesimal sinusoidal variations in the jet radius R, provided that the wavelength of perturbation exceeded a critical minimum value, $\lambda_{min} = 2\pi R$. Rayleigh demonstrated that growth kinetics favored a wavelength exceeding λ_{min}, one that optimized the interplay between surface energy reduction and transport distance. Rapid growth of perturbations with this kinetically preferred wavelength, λ_{max}, was expected to transform an initially continuous jet into a series of discrete droplets with a spacing of $\approx \lambda_{max}$.

These concepts were extended by Nichols and Mullins[3] to describe the morphologic evolution of both solid rods and of cylindrical pores in solids with isotropic surface energy. Their analysis showed that the kinetically dominant wavelength was sensitive to the transport mechanism dominating perturbation-amplitude growth. For infinitely long cylindrical pores,

their analysis showed that surface-diffusion-dominated evolution would result in a kinetically favored wavelength of $\sqrt{2} \cdot \lambda_{min}$ ($\approx 8.89R$). For volume-diffusion-controlled evolution, a longer wavelength, $\approx 12.96R$, emerged as kinetically dominant.

Cahn[4] considered the impact of surface energy anisotropy on Rayleigh instabilities, and demonstrated that λ_{min} would shift if surface reorientation during perturbation growth changed the surface energy γ. Cahn treated an idealized cylindrical body in which γ was isotropic in a plane normal to the cylinder axis (yielding a circular cross section) but that varied in response to axial perturbations. His analysis showed that if γ is in a local minimum for an unperturbed cylinder then $\lambda_{min} > 2\pi R$, whereas if γ decreases with perturbation, then $\lambda_{min} < 2\pi R$. Thus, for channels bounded by stable or equilibrium surfaces, an increased resistance to perturbation growth would arise, while for channels bounded by higher-energy unstable surfaces, growth of shorter wavelength perturbations was possible. More recent work has examined cylinders in which the anisotropy has either cubic or uniaxial symmetry.[5]

Stölken and Glaeser[6] extended the kinetic analysis of Nichols and Mullins to the idealized system treated by Cahn, and showed that for surface-diffusion-controlled instability of pore channels, the kinetically favored wavelength remained $\sqrt{2} \cdot \lambda_{min}$. However, since λ_{min} is now a surface-energy-anisotropy-dependent parameter, it is evident that λ_{max} should be orientation-dependent in crystalline materials (with orientation-dependent surface energies). More detailed assessments of evolution kinetics for model anisotropic systems can be found in the literature.[7, 8]

Analyses of Rayleigh instabilities during high-temperature crack healing provide an attractive tracer-free method of assessing the surface diffusivity. During intermediate-stage crack healing, cylindrical pore channels form and subsequently break up into strings of isolated pores. Crack-healing experiments in sapphire by Yen and Coble,[9] and by Gupta[10, 11] were interpreted in the context of the analysis for isotropic systems formulated by Nichols and Mullins. Rödel[12] was the first to use lithographic processing methods to generate pore channels with controlled geometry and crystallography, and thus provided the first unambiguous evidence of significant surface-energy-anisotropy effects on Rayleigh instabilities. Subsequent work by Powers[13, 14] examined effects of dopants on Rayleigh instabilities in sapphire; impurity-specific and crystallography-specific shifts in λ_{max} were reported. Kulinsky *et al*.[15] extended the method to examine the evolution of pore channels with imposed perturbations of controlled wavelength and amplitude, and demonstrated agreement with the general predictions for the kinetics of pore breakup in anisotropic systems. Powers[16] provided the most comprehensive assessment of pore channel orientation on morphologic stability to date, examining the spatial and temporal evolution of arrays of pore channels with their axes lying within the **c** plane of sapphire, and their in-plane direction systematically varied. His results showed clear evidence of strong variations in λ_{max} as the channel orientation varied.

Kitayama[17] examined the morphologic evolution of 20 µm × 20 µm × 0.5 µm pores in sapphire. Those with the 20 µm × 20 µm face parallel to the **c** plane evolved much more slowly than those of similar geometry but with their large faces parallel to the **m** plane. It has been demonstrated that the **c** plane is part of the equilibrium shape of sapphire at both 1600°C and 1800°C, and that the **m** plane is not stable at either 1600°C and 1800°C. More generally, an abundant body of work,[17-20] spanning a wide range of temperature, material purity, and ambient atmosphere has shown that the **m** plane is not a component of the equilibrium shape of sapphire. As a result, a comparison of the evolution behavior of pore channels lying parallel to the **c** and **m**

planes was expected to highlight the influence of variations in the bounding-surface stability on evolution energetics and kinetics.

EXPERIMENTAL PROCEDURES

The general experimental procedures involved in developing microdesigned internal defect structures by lithographic methods have been described in several review papers.[21, 22] A brief summary is provided here with details appropriate to the present experiments.

Optical-grade, 99.996% pure, $1.00'' \times 1.00'' \times 0.020''$ sapphire crystals with the large surface within $\pm 1°$ of $\mathbf{m}(10\bar{1}0)$ were acquired from Crystal Systems, Inc.. The surface orientation and in-plane directions were determined by Laue backscatter x-ray diffraction. The crystals were cut into four equal pieces using a low-speed diamond saw. Fiduciary marks were made on one side of the crystal pieces to facilitate crystal alignment during diffusion bonding.

Photolithography and ion milling were performed in a Class 100 clean room. Standard cleaning procedures designed to remove organic and metallic impurities from the surface were used prior to application of an ≈ 1.8-μm-thick layer of photoresist (Shippley 1818). Following a bake of the resist-coated substrate, a mask pattern was selectively exposed using a Canon 4× projection mask aligner. The portion of the pattern relevant to the present results is shown in Figure 1a. The starburst pattern with circular arrays of high-aspect-ratio channels is repeated four times in the mask. The 24 channels are rotated in 15° increments, thereby sampling 12 distinct crystal orientations. The etched channel width is 3 μm. An attempt was made to align the mask such that sets of channels would lie parallel to the <0001> and the <11$\bar{2}$0> directions.

The exposed resist was developed for 1 min in Microposit Developer Concentrate diluted 1:1 with deionized water. The sapphire was rinsed in deionized water, dried with a nitrogen gun, and baked for 30 min in an air oven at 90° C. Satisfactory patterns resulting from this procedure were set aside for ion milling. For each milled piece of sapphire, another piece of unmilled sapphire, cut from the same original $1'' \times 1''$ crystal, was set aside for diffusion bonding.

The sapphire with patterned photoresist was milled with Ar ions for 45 min in a Veeco Microetch System ion mill. The depths of the etched features (90 nm) were measured with an Alpha-Step IQ Surface Profiler. Crystals were recleaned with solvents, and then annealed in air for a minimum of 2 h at 600°C in a covered, high-purity alumina crucible.

An etched and an unetched surface of a pair of substrates cut from the same wafer were brought into contact, and aligned (using the fiducial marks) to assure that common in-plane directions were oriented parallel to one another. BN spacers were used to separate the external substrate surfaces from graphite foil and rams in the vacuum hot press. Assemblies were diffusion bonded for 10 h at 1350°C under an applied pressure of 10 MPa. Successful bonding resulted in a crystal with the etched features from the photolithography transformed into internal cavities lying on a low-angle (typically $\leq 1°$) twist grain boundary as shown in Figure 1b.

The bonded assemblies were annealed at 1700°C in a vacuum furnace ($<3 \times 10^{-5}$ torr). The heating and cooling rate of the furnace was 30°C/min; indicated anneal times reflect the total time at 1700°C. Bonded crystals were annealed until the etched channels had evolved into approximately equiaxed pores that were stable to further break up. A total of 24 anneals were conducted. Since sapphire is transparent, observation of the evolution of internal cavities by visible-light microscopy between anneals was possible. The total anneal time was 604 h.

The crystals were examined after bonding and after each anneal in reflected- and dark-field mode using a Zeiss visible-light microscope. Determinations of the average pore spacing
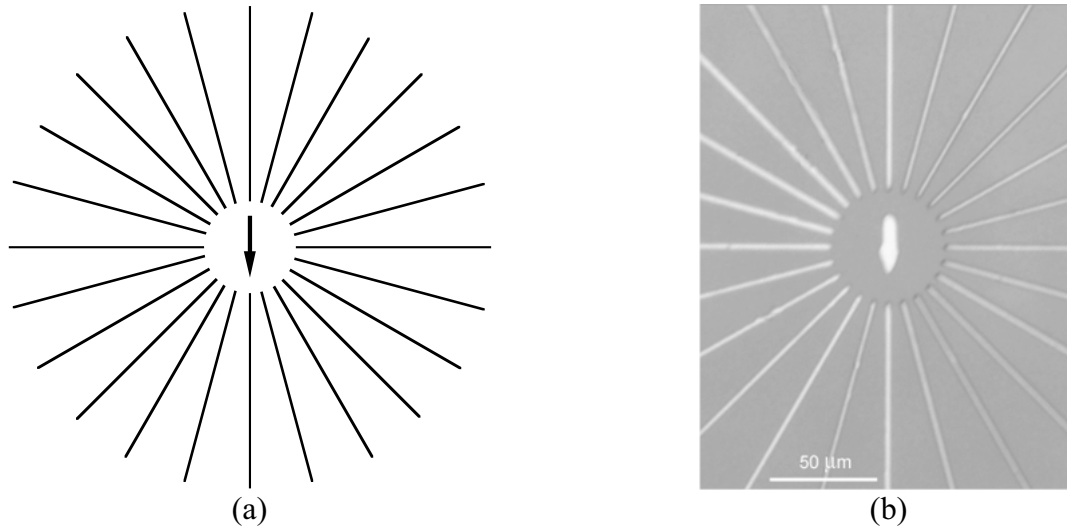
Figure 1   a) Schematic illustration of pore-channel array, and b) internalized pore channels after bonding, but prior to annealing at 1700°C.

for each channel orientation were done using the photomicrographs generated after each anneal. Average values for multiple channels are reported.

RESULTS & DISCUSSION

After bonding, but prior to any high-temperature annealing, the pore channels are much wider (3 µm) than they are deep (90 nm). Consistent with observations in prior work, the very initial stages of annealing are marked by an apparent narrowing of the channels as the initially broad and shallow cross section, becomes more equiaxed. Figures 2a and 2b show channels after 20 min and 60 min total annealing at 1700°C, respectively. The extent of shape adjustment is apparent by comparing the channels immediately after bonding (Figure 1b) with and after the
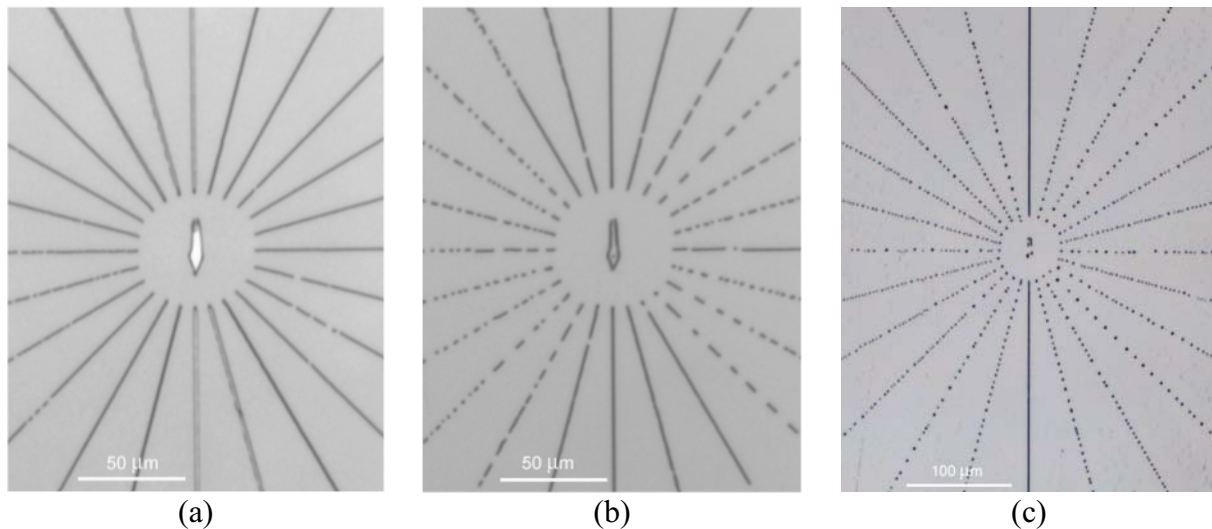

Figure 2   Optical micrographs of pore-channel array annealed at 1700°C for a total duration of a) 20 min, b) 60 min, and 480 min. The region shown is the same in the three images. The vertical channels are parallel to $[11\bar{2}0]$.

first 20-min anneal (Figure 2a). In Figure 2a, it is also apparent that the channels rotated 15º counterclockwise from vertical have developed roughly sinusoidal perturbations along their edges. The development of axial perturbations is not visible in all of the channels at this magnification. After only 60 min of total anneal time at 1700°C, the break up of channels in certain orientations is already nearing completion as shown in Figure 2b. Other channels, most notably those oriented along the [11$\bar{2}$0] direction (oriented vertically in all the images), evolve more slowly.

Both the evolution wavelength and the rate of evolution can be profoundly affected when stable facets bound the pore channel. In all cases, the as-etched channel geometry is primarily bounded by unstable **m**(10$\bar{1}$0) planes. The **m** planes break down into **r**{$\bar{1}$012}- and **s**{10$\bar{1}$1}- facets of very fine scale, producing a "rough" surface. This breakup can also provide an easy path for the formation of perturbations along the length of the channel. For channels oriented along the [11$\bar{2}$0] direction it is possible that **c**-, **r**-, and **s**-facets completely bound the channel; all three facets are part of the equilibrium shape. Although the etched channels presumably do not start with any sides of these orientations, the channels may have an easy path to these facets and it is reasonable to believe that the presence of faceted surfaces will stabilize a channel. Facet displacements required for perturbation growth may then be difficult. For stable facets, these displacements may require the nucleation of atomic height patches and cavities on a normally stable surface with an attendant nucleation barrier, as discussed by Mullins and Rohrer.[23] Complete breakup of [11$\bar{2}$0]-oriented channels was not seen until the anneal time had reached 604 h. This indicates that surface energy anisotropy can be a powerful ally in efforts to retain fine-scale structures. The edges of channels pointed in the [0001] direction could be stabilized by **a**{11$\bar{2}$0}-plane facets, but there are indications that the **a** plane is only marginally stable and may in fact be above its roughening temperature at 1700°C. In contrast, for most other channel orientations, a stepped structure may develop along the channel edges that provides multiple attachment and detachment sites.

Pore spacings, λ, were measured as a function of pore-channel orientation, and assumed to reflect λ_{max}. λ_{max} is expected to scale with the pore-channel radius. In order to compare the results of this experiment with those of other experiments where the pore channels had slightly different dimensions, it is convenient to report the result in terms of a pore spacing normalized by the channel radius. Channels resulting from the microlithography and bonding process initially have a very flattened cross section, not well described by a circular radius. However, shape equilibration in very early stages of annealing leads to a more equiaxed cross section, one that may be described by an equivalent radius, R, calculated from the initially determined cross sectional area of the channel. Figure 3a is a polar plot indicating the variation of the average normalized pore spacing (λ/R) with orientation for pore channels in the **m** plane. The values given are averaged from channels in four separate "starbursts" sharing the same orientation. For all orientations, the observed values of λ/R exceed those expected for an isotropic solid. Channels oriented parallel to [11$\bar{2}$0] in the **m** plane are the most resistant to break-up by a wide margin, and also exhibit the largest λ/R values. Channels of this orientation were also present in prior studies of **c**-plane sapphire by Powers,[16] and also found to be the most resistant to breakup, as shown in Figure 3b. As evident by comparing Figures 3a and 3b, for channels not parallel to [11$\bar{2}$0], the observed values of λ/R in the **m** plane tend to be much less than those of channels in the **c** plane of sapphire.

The impact of these wavelength differences of evolution kinetics can be clearly seen when pore arrays in the **m** plane and **c** plane of sapphire are compared. Figures 4a and 4b
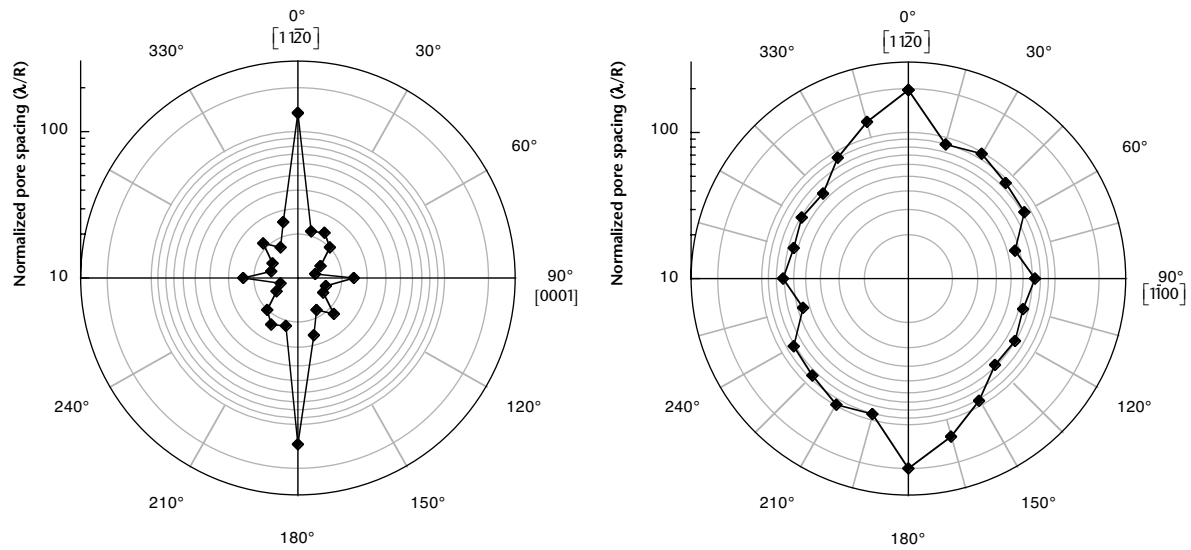
Figure 3　　Polar plot of normalized pore spacings (λ/R) as a function of the pore channel axis orientation within a) the **m**$(10\bar{1}0)$ plane, and b) the **c**(0001) plane.
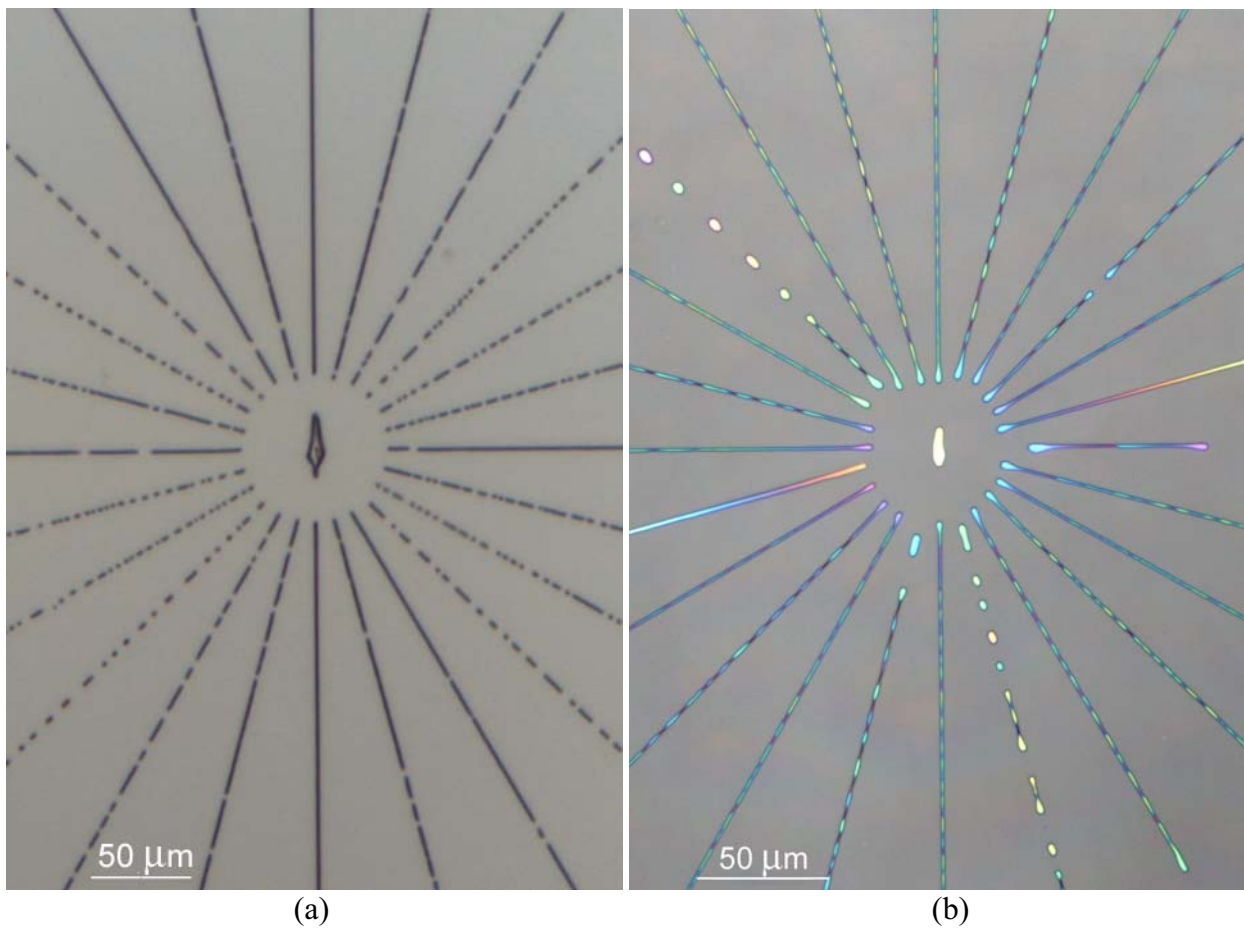

(a)　　　　　　　　　　　　　　　　　(b)

Figure 4　　Optical micrographs of pore channels a) after 1 h at 1700°C for an **m**-plane sample, and b) after 146 h at 1700°C for a **c**-plane sample.

compare the behavior of geometrically similar pore channels in **m**-plane and **c**-plane sapphire, respectively. It is clear that for many orientations, breakup is complete in the **m-**plane sample. In contrast, while the majority of the **c**-plane channels have well-developed perturbations but are still continuous. It is notable that the **c**-plane sample has been annealed for 146(!) h at 1700°C while the **m**-plane sample has only been annealed for 1 h at 1700°C. Clearly, the increase in transport distance that accompanies an increase in λ has a substantial retarding effect on breakup, consistent with modeling predictions. A more detailed analysis of the kinetics in the context of available models for anisotropic systems is in progress, and results will be published elsewhere.

SUMMARY & CONCLUSIONS

The use of microlithographic methods in conjunction with ion-beam etching and solid-state diffusion bonding allows the fabrication of microdesigned internal defect structures. Crackline flaws, pores, and pore channels generated in this fashion have controlled geometry and cyrstallography, and therefore provide an ideal vehicle for model studies of morphologic instability. The impact of surface energy anisotropy on evolution directions and rates can be determined. A strong effect of surface energy anisotropy is implied the morphologic evolution of pore channels introduced into both stable (**c**) and unstable (**m**) planes of sapphire. Features fully bounded by stable surfaces, those that are part of the Wulff shape, are most strongly stabilized. This stabilization manifests itself both in the spatial and temporal characteristics of evolution. The periodicity or wavelength of pore channel breakup shifts to wavelengths that far exceed those expected for Rayleigh instabilities in materials with isotropic surface energy. As a result of the increased transport distance associated with breakup, the evolution rate is strongly decreased. The associated increases in feature "lifetime" are significant, and suggest that the use of surface energy anisotropy may play an important role in stabilizing fine-scale structures.

ACKNOWLEDGMENTS

REFERENCES

1.   M. T. Plateau, "On the recent theories of the constitution of jets of liquid issuing from circular orifices," *Philosophical Magazine S4*, **12**, [79], 286-97 (1856).
2.   L. Rayleigh, "On the Instability of Jets," *Proceedings of the London Mathematical Society*, **10**, 4-13 (1879).
3.   F. A. Nichols and W. W. Mullins, "Morphological Changes of a Surface of Revolution due to Capillarity-Induced Surface Diffusion," *J. Appl. Phys.*, **36**, [6], 1826-35 (1965).
4.   J. W. Cahn, "Stability of rods with anisotropic surface free energy," *Scr. Metall.*, **13**, [11], 1069-71 (1979).

5.   K. F. Gurski and G. B. McFadden, "The effect of anisotropic surface energy on the Rayleigh instability," *Proc. Roy. Soc. of London Series A*, **459**, [2038], 2575-98 (2003).

6.   J. S. Stölken and A. M. Glaeser, "The Morphological Evolution of Cylindrical Rods with Anisotropic Surface Free Energy via Surface Diffusion," *Scripta Metall. et Mater.*, **27**, [4], 449-54 (1992).

7.   A. M. Glaeser, "A New Approach to Investigating Surface Transport in Ceramics," in MASS AND CHARGE TRANSPORT IN CERAMICS, vol. 71, *Ceramic Transactions*, K. Koumoto, L. M. Sheppard, and H. Matsubara, Eds. Westerville: The American Ceramic Society, 1996, pp. 117-36.

8.   A. M. Glaeser, "Model Studies of Rayleigh Instabilities via Microdesigned Interfaces," *Interface Science*, **9**, [1/2], 65-82 (2001).

9.   C. F. Yen and R. L. Coble, "Spheroidization of Tubular Voids in α-Al_2O_3 crystals at high temperatures," *J. Am. Ceram. Soc.*, **55**, [10], 507-9 (1972).

10.   T. K. Gupta, "Instability of cylindrical voids in alumina," *J. Am. Ceram. Soc.*, **61**, [5-6], 191-5 (1978).

11.   T. K. Gupta, "Crack Healing in Al_2O_3, MgO, and Related Materials," in ADVANCES IN CERAMICS, vol. 10, W. D. Kingery, Ed. Columbus: The American Ceramic Society, 1984, pp. 750-66.

12.   J. Rödel and A. M. Glaeser, "High-Temperature Healing of Lithographically Introduced Cracks in Sapphire," *J. Am. Ceram. Soc.*, **73**, [3], 592-601 (1990).

13.   J. D. Powers and A. M. Glaeser, "High-Temperature Healing of Cracklike Flaws in Mg- and Ca-Ion-Implanted Sapphire," *J. Am. Ceram. Soc.*, **75**, [9], 2547-58 (1992).

14.   J. D. Powers and A. M. Glaeser, "High-Temperature Healing of Cracklike Flaws in Titanium Ion-Implanted Sapphire," *J. Am. Ceram. Soc.*, **76**, [9], 2225-34 (1993).

15.   L. Kulinsky, J. D. Powers, and A. M. Glaeser, "Morphological Evolution of Pre-perturbed Pore Channels in Sapphire," *Acta Mater.*, **44**, [10], 4115-30 (1996).

16.   J. D. Powers and A. M. Glaeser, "Orientation effects on the high-temperature morphological evolution of pore channels in sapphire," *J. Am. Ceram. Soc.*, **83**, [9], 2297-304 (2000).

17.   M. Kitayama, T. Narushima, and A. M. Glaeser, "The Wulff shape of alumina. II. Experimental measurements of pore shape evolution rates," *J. Am. Ceram. Soc.*, **83**, [10], 2572-83 (2000).

18.   J. R. Heffelfinger, M. W. Bench, and C. B. Carter, "On the faceting of ceramic surfaces," *Surf. Sci. (Netherlands)*, **343**, [1-2], L1161-6 (1995).

19.   J. R. Heffelfinger and C. B. Carter, "Mechanisms of surface faceting and coarsening," *Surf. Sci. (Netherlands)*, **389**, [1-3], 188-200 (1997).

20.   M. Kitayama and A. M. Glaeser, "The Wulff shape of alumina. III. Undoped alumina," *J. Am. Ceram. Soc.*, **85**, [3], 611-22 (2002).

21.   J. Rödel and A. M. Glaeser, "Microdesigned Interfaces: New Opportunities for Materials Science," *Yogyo Kyokai Shi*, **99**, [4], 251-65 (1991).

22.   M. Kitayama, J. D. Powers, L. Kulinsky, and A. M. Glaeser, "Surface and interface properties of alumina via model studies of microdesigned interfaces," *Journal of the European Ceramic Society*, **19**, [13-14], 2191-209 (1999).

23.   W. W. Mullins and G. S. Rohrer, "Nucleation barrier for volume-conserving shape changes of faceted crystals," *J. Am. Ceram. Soc.*, **83**, [1], 214-16 (2000).